IEEE Photonics Journal
An IEEE Photonics Society Publication

Open Access

Hybrid Optical Wireless Network for Future SAGO-Integrated Communication Based on FSO/VLC Heterogeneous Interconnection

Volume 9, Number 2, April 2017

Zhitong Huang
Zhenfang Wang
Minglei Huang
Wei Li
Tong Lin
Peixuan He
Yuefeng Ji

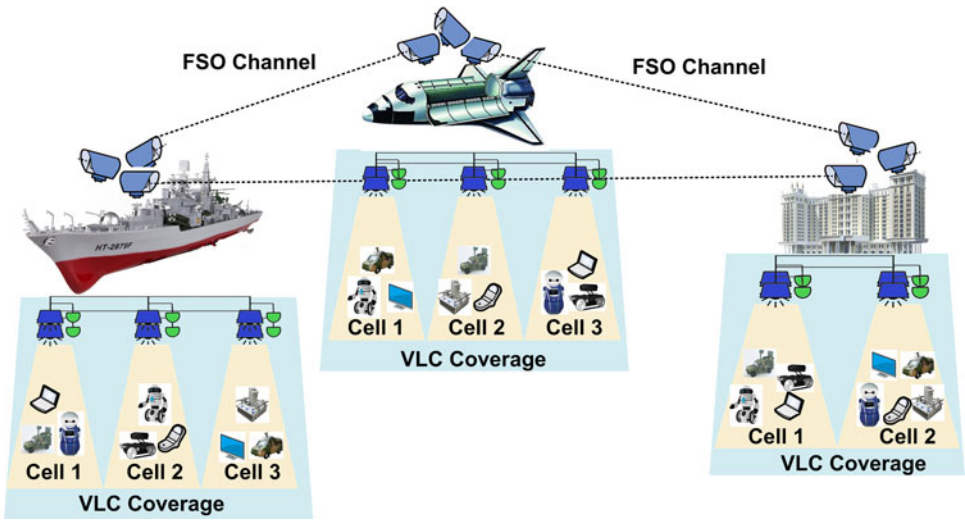

DOI: 10.1109/JPHOT.2017.2655004
1943-0655

IEEE photonics SOCIETY

IEEE

Hybrid Optical Wireless Network for Future SAGO-Integrated Communication Based on FSO/VLC Heterogeneous Interconnection

Zhitong Huang,[1,2] Zhenfang Wang,[1] Minglei Huang,[1] Wei Li,[1] Tong Lin,[1] Peixuan He,[1] and Yuefeng Ji[1,2]

[1]State Key Laboratory of Information Photonics and Optical Communications, Beijing University of Posts and Telecommunications, Beijing 100876, China
[1]Beijing Advanced Innovation Center for Future Internet Technology, Beijing University of Technology, Beijing 100124, China

DOI:10.1109/JPHOT.2017.2655004

Manuscript received December 22, 2016; revised January 8, 2017; accepted January 15, 2017. Date of publication January 18, 2017; date of current version March 10, 2017. This work was supported in part by the National 973 Program (No. 2013CB329205) and in part by the National Natural Science Foundation of China (No. 61401032), Funds of Beijing Advanced Innovation Center for Future Internet Technology of Beijing University of Technology, China. Corresponding author: Z. Huang (e-mail: hzt@bupt.edu.cn).

Abstract: Free-space optics (FSO) and visible light communication (VLC) share the same optical wireless features, such as high data rate, license free, energy efficient, flexible access, and high degree of security. A hybrid optical wireless network based on FSO/VLC heterogeneous interconnection is presented here for future space-air-ground-ocean-integrated communication architecture, especially in the radio-frequency-sensitive (RF) or security-required environments. The functional modules of the hybrid network coordinator are defined, along with the implementation and deployment details. Three fundamental network-layer mechanisms are designed in the coordinator including user identification and localization, user mobility and handoff control, and routing and traffic management. An experimental platform is built to evaluate the transmission performance of the presented hybrid network, and a complete data aggregation/transmission/distribution procedure based on heterogeneous interconnection is first realized, which includes two-segment 1.0-m 450-Mb/s orthogonal-frequency-division-multiplexing-based VLC transmissions interconnected by one-segment 430-m 0.96-Gb/s on-off keying (OOK)-based nonturbulent FSO transmission, with the bit error rate under the forward-error-correction limit (3.8×10^{-3}). The VLC transmission performances under three speed levels and FSO transmission performances under five typical air-quality conditions are experimentally demonstrated, which validate the feasibility of the proposed hybrid optical wireless network.

Index Terms: Free-space optics (FSO), visible light communication (VLC), heterogeneous interconnection, hybrid optical wireless network, space-air-ground-ocean (SAGO)-integrated communication.

1. Introduction

Conventional radio-frequency-based wireless communication has achieved tremendous developments over the past two decades, which satisfies the ubiquitous communication requirements and thus, significantly improves the quality of modern life. However, its ability to further advance the

information society is now seriously challenged by the overcrowding radio-frequency (RF) spectrum, leading to insufficient capacity to support the ever-increasing wireless data traffic [1]. The idea of optical wireless communication (OWC) has been presented as a promising solution for developing higher optical spectrum and obtaining larger bandwidth [2]–[4].

As the traditional realization of OWC, the free space optics (FSO), which utilizes the coherent lightwave of the laser diode (LD) to transfer information in free space, is an attractive technology due to its advantages such as high data-rate, license- free, long distance, high energy efficiency, reduced interference, high degree of security and privacy [5], [6]. Although the FSO is still facing several technical difficulties in terms of atmospheric turbulence, transceiver alignment, and ambient light, yet it has been widely suggested to be an important candidate for the future broadband wireless technology not only for terrestrial applications but also for spatial and underwater scenarios [7], [8].

On the other hand, due to the large-scale deployment of the white light-emitting-diode (LED) as the next-generation green lighting, the visible light communication (VLC), which utilizes the incoherent lightwave of LED to transfer information in wireless channel, has been presented [9], [10] as a popular solution for short-distance broadband wireless communication. With the progresses of advanced modulation, equalization and multiplexing schemes for the VLC system [11]–[13], along with the manure of the corresponding integrated-circuit chips [14], more research interests have been moved to the network-layer mechanisms such as cell construction, multi-user access, and outdoor interconnection [15], [16].

Although the light sources, and thus the system modeling methodologies of the FSO and VLC systems are different, the same advantages of optical wireless features make it possible to integrate these two technologies into a hybrid optical wireless network, which is preferable to be deployed in the RF-sensitive environments and the security communication situations. Currently, the wireless communication is required not only for the terrestrial applications, but also extended more to the deep-space, deep-ocean and deep-ground situations, in which such hybrid optical wireless network will play an important role.

The heterogeneous interconnections between optical wireless communication and other technologies have been widely discussed in the literature. The FSO is always a popular candidate to be integrated with the fiber-based passive optical network (PON) to realize the last-mile optical flexible access, while nowadays more attention has been paid to the FSO- based back-haul transmission in mobile network [17], and the channel analysis of mixed RF/FSO systems [18], [19]. On the other hand, since the signals are carried by the driven current of the LED devices in VLC system, it is an intrinsic scheme to integrate the VLC system with the power-line communication (PLC) system [20], however, in order to advance the system capacity and show the spectrum advantages of VLC, the PON will be more suitable for integration [21]. The uplink scheme and the channel occlusion are two important problems in VLC network, due to the illumination constraint and line-of-sight feature respectively, and the combination of mixed RF/VLC systems can solve these problems [22]. Furthermore, with the widely-spread of the idea of the fifth generation (5G) as the future mobile technology, many interests have been moved to embed VLC into the 5G framework [23], [24]. A system-level OWC interconnection is presented in [25] which utilize a single mode fiber to connect the outdoor FSO and the indoor VLC system. In summary, current researches on heterogeneous OWC are mainly focusing on the system-level interconnection, especially on the optical wireless and the RF integration. In this paper, however, we concentrate on designing a hybrid optical wireless network, along with the implementation details of network-layer functional modules. To the best of our knowledge, it is the first time in this paper to experimentally demonstrate a direct FSO/VLC heterogeneous interconnection with the data aggregation and distribution, which validates the feasibility of the proposed hybrid network architecture.

2. Hybrid Optical Wireless Network Architecture

Fig. 1 presents the application scenarios for the proposed hybrid optical wireless network architecture. Such architecture is quite suitable to be deployed for the broadband wireless communication in RF-sensitive and security-required situations, especially in the deep-space, deep-ocean and

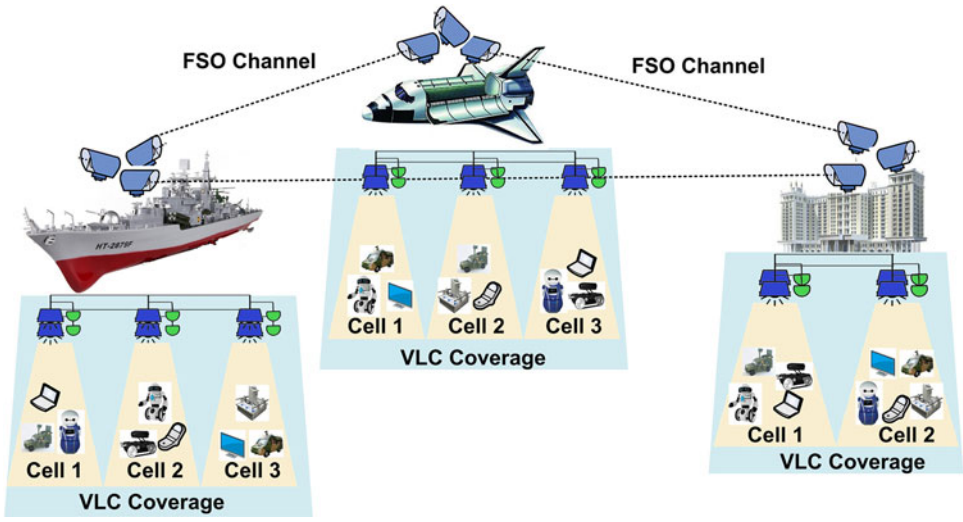

Fig. 1. Typical application scenario for the hybrid optical wireless network architecture.

deep-ground environments of future space-air-ground-ocean (SAGO) integrated communication. Fig. 1 shows the FSO-based inter-communication and VLC-based intra-communication among different RF-sensitive cabins, in which we select the spacecraft in the deep-space, the submarine in the deep-ocean, and the command post in the deep-ground as three typical examples. The inter-communications among different cabins require long-distance and large-bandwidth, so we utilize the FSO technology, and the optical acquisition-pointing-tracking (APT) modules are required due to the continuous movements of the cabins. Inside the cabins, the VLC technology is deployed to realize the short-distance high-speed wireless communication. A VLC multi-cell structure is naturally formed according to the distribution of the LED devices, and different user terminals (such as robots, intelligent vehicles, computers, etc.) access the network using the bi-directional VLC transceivers embedded in the terminals and the ceiling of the cabins. Within each VLC cells, the downlink data is broadcasted in which different terminals share the downlink channel in time-division- multiplexing (TDM) manner, and the time-division-multiple-access (TDMA) technique is accordingly implemented in the uplink direction.

Three kinds of communication modes can be defined in such hybrid optical wireless network. The first one is the communication between different terminals within the same VLC cell inside one cabin. Considering the limited coverage of a single VLC cell, the VLC-based device-to-device (D2D) technology is suggested for this mode [26], [27], which can also save more valuable bandwidth for the other two modes. The second mode is the communication between terminals in different VLC cells inside the same cabin. Since no line-of-sight (LOS) channel can be used for this mode, two bi-directional VLC channels (uplink and downlink) in different cells should be involved in such mode, which will be operated by the heterogeneous network (HetNet) management system, defined as the FSO/VLC HetNet coordinator here. Moreover, if the terminal moves out of the original cell in this mode, a handoff mechanism should be generated to maintain the communication. The third mode is the communication between terminals in different VLC cells of different cabin. Two bi-directional VLC channels and one bi-directional FSO channel will be involved in such mode, which will be operated and controlled by two HetNet coordinators in different cabins.

The FSO/VLC HetNet coordinator is the key element for the proposed network, which is mainly responsible for the data interconnection, aggregation and distribution, signaling interaction and resource scheduling. Fig. 2 presents the functional modules of this coordinator, which can be divided into three parts: the VLC-transmission-control part at the bottom, the FSO- transmission-control part at the top, and the distinctive HetNet-control part in the middle. Each coordinator is

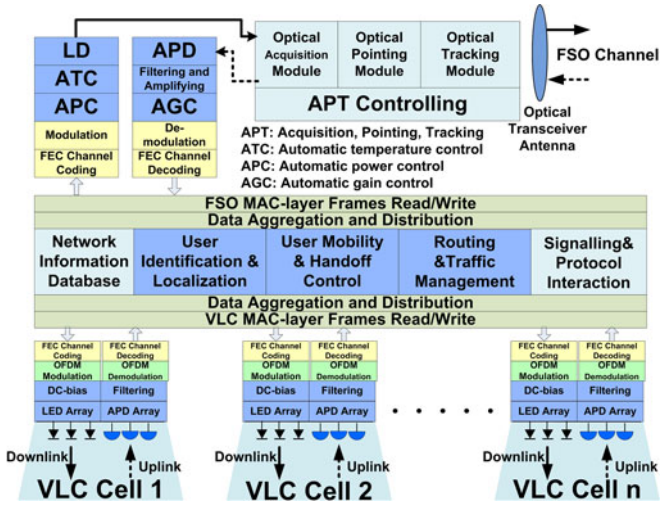

Fig. 2. Functional modules of the FSO/VLC HetNet coordinator.

responsible for all the communications within the scale of one cabin, especially the second modes and the third modes.

In the VLC-transmission-control part, the LED transmitting array and the avalanche-photo-diode (APD) receiving array are deployed at the ceiling of the cabin, realizing the electrical-optical conversion of the downlink signal and the optical-electrical conversion of the uplink signal respectively. The received analog electrical signals are amplified, filtered, and transferred to digital signals by the adaption circuits, and then sent to digital-signal-processing (DSP) module for the demodulation and decoding procedures (the downlink operations are in the opposite order of the uplink operations). The orthogonal frequency division multiplexing (OFDM) modulation, along with the hybrid time-frequency-domain equalization [12] is recommended to realize the high-speed VLC transmission. In the FSO-transmission-control part, different modulation mechanisms can be selected, which is decided by the required capacity for aggregated service data inside the VLC cells. If the aggregated data is less, the simple on-off keying (OOK) modulation can satisfy the speed requirement, whereas if the aggregated data is large or there are many VLC cells within one cabin, more complicated modulation such as OFDM will be used to enhance the FSO channel speed. The automatic-temperature-control (ATC) and automatic-power-control (APC) modules are required in the LD transmitter since the semi-conductor is degradation-sensitive and temperature-sensitive, and the automatic-gain-control (AGC) module is required in the receiver to adapt the change of the channel characteristics. As the cabins are always keeping on moving, the acquisition-pointing-tracking (APT) module should be embedded in the FSO transceivers to maintain the communication. There is only one FSO transceiver presented in Fig. 2, but actually, more FSO transceivers are required in the HetNet coordinator since one cabin are usually communicating with several cabins simultaneously within the SAGO-integrated communication in practical applications, shown in Fig. 1.

After the media-access-control (MAC) layer operations, the service data from the transmission-control parts will be transmitted to the middle HetNet-control module, which is the vital part of the coordinator. The basic function of the HetNet-control module is to realize the data aggregation and distribution between the outside FSO and the inside VLC networks and such operations is controlled by three important network-layer algorithms implemented in the coordinator: user identification and localization, user mobility and handoff control, and the routing and traffic management.

Firstly, each terminal in the hybrid network should have a unique ID to realize efficient addressing. The basic method for identification is to set a global ID number to each terminal, which is unique throughout the whole network, but with the increasing of the cell number and the terminal

number, the searching and maintenance of the global ID database will be low-efficient; therefore, a hierarchical numbering mechanism should be introduced. According to the order of addressing, a four- level hierarchical numbering scheme can be used which sequentially contains the cabin ID, VLC cell ID, terminal type ID and terminal ID. However, the VLC cell ID may change due to the movement of terminal, so it is inconvenient to be included in the global ID. Therefore, a three-level global ID is defined here containing cabin ID, terminal type ID and terminal ID. User localization is required for implementing data distribution, which is realized by the positioning algorithms. There are basically two categories of localization mechanisms, the rough localization which only determines the cell ID in which the user locates, and the accurate localization which presents the specific terminal position within the cell. The distribution of the VLC cells in the cabin decides whether the rough or the accurate positioning is selected. If the LED lights are deployed separately in the cabin, and therefore the VLC cells are non-overlapped, the rough localization is enough to accomplish the correct data distribution. If the LED lights are deployed intensively in the cabin to realize the uniform illumination, and therefore the VLC cells are overlapped, the accurate localization should be introduced [28] not only for exact positioning in the overlapping area but also for the handoff procedure. In this paper, a practical cell formation scheme is recommended in the hybrid network [29] which utilizes the walls and partitions within the cabin to naturally construct separate VLC cells and a signaling- based rough positioning mechanism can be adopted. The terminal locations will be stored in the database and dynamically updated by the positioning module, and the coordinator searches the database to obtain the VLC cell ID of the user terminal and then accomplishes the data distribution.

Second, if the cross-cell movement occurs in the cabin, the user mobility and handoff module will be generated. The selection of the handoff mechanisms is decided by the user QoS requirements, along with the cell distribution manners. The hard handover scheme is suitable for separate cell distribution, in which the service will pause for a while when the terminal moves into the dark area and then be restored by the signaling interaction in the new cell. In the presented separate-cell scenario, an active-handoff mechanism can be utilized [30] to reduce the handoff latency, which is realized with the assistant of the accurate positioning. If the VLC cells are overlapped, the soft handoff procedure can be accomplished based on the localization and tracking algorithms.

Thirdly, the coordinator implements routing calculation and traffic management algorithms which select the optimal path for the service data considering the real-time distribution of the network traffic and the available channel bandwidth on each FSO links. In the presented hybrid network, all the second-mode communications within one cabin is controlled by the centralized coordinator, so routing operations will only be used for the third-mode communications.

The above three network-layer mechanisms of the coordinator are implemented by interactions of the signaling messages, which should be defined in the network protocols. The network information databases are also required, which contain the information of the terminals, network traffic, and the link resources.

3. Experiment Platform

To validate the feasibility of the proposed hybrid network architecture, we build a FSO/VLC heterogeneous interconnection platform, shown in Fig. 3, which accomplishes a uni-directional third-mode communication between two VLC cells deployed in different locations. The network-layer mechanisms and the physical-layer data aggregation/distribution procedures are the two key elements for the proposed hybrid network architecture. Due to the experimental condition limitations, we select the minimum collection of the functional modules defined in Fig. 2 to measure the transmission performance of the hybrid network architecture, which includes the FSO/VLC optical transceiver devices, electrical adaption circuits, modulation modules, along with the data aggregation and distribution modules. However, the APT modules, the forward error correction (FEC) encoding module, along with the network-layer modules are not included in current experiment platform, and we will improve our platform and evaluates the other physical-layer and network-layer mechanisms in the future.

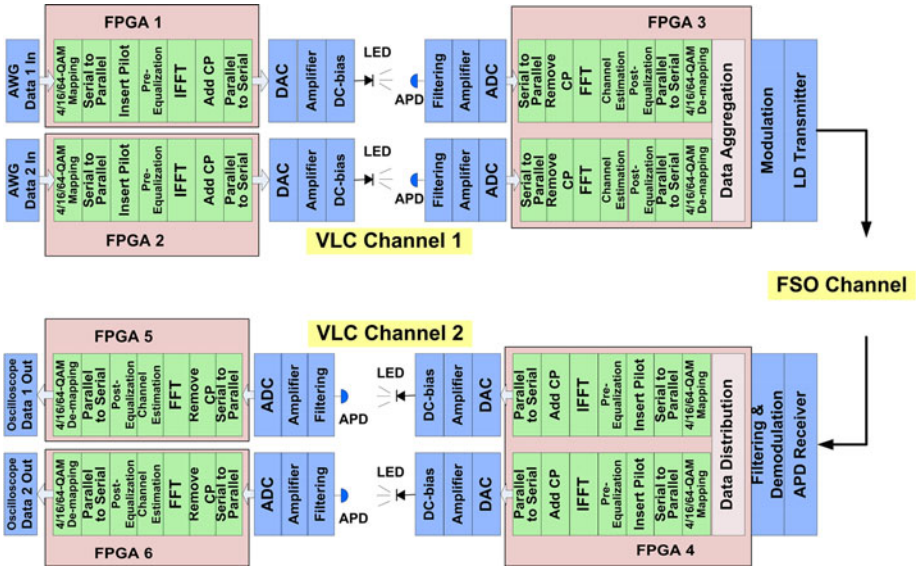

Fig. 3. Diagram of the FSO/VLC heterogeneous interconnection experimental platform.

In the experiment platform, two columns of pseudo-random data sequences are generated by the arbitrary-waveform- generator (AWG, Tektronix AWG5012) to represent the baseband digital signals from two VLC user terminals. The data sequences are then sent into the DSP modules for the first-segment OFDM-based VLC transmission (VLC channel 1), whose block diagram is shown in Fig. 3. The quadrature amplitude modulation (QAM) is used for high-order data mapping, and the serial to parallel operation is used for sub-carrier loading. The pilot is inserted for channel estimation, and the pre-equalization is implemented in the frequency-domain to compensate the linear distortion. The Hermitian symmetry of complex signals is used before inverse fast Fourier transform (IFFT) to produce a real time domain output signal, and the clicks prefix (CP) is added to mitigate inter-symbol interference. After the parallel to serial operation and the digital-to-analog conversion, the OFDM signal will then be uploaded on the DC-bias to modulate the LED. In the platform, a LED lamp which contains seven LED chips (Cree PLCC4) is used for VLC transmitter. At the receiver, a commercially available APD (Hamamatsu, S8664-20K) is used to detect the optical signals, and the received signal is filtered and amplified by a low noise PA (Mini-Circuits ZFL-1000LN+) and then sent into the DSP module for OFDM demodulation, in which a time-domain post-equalization is carried out to mitigate the nonlinear distortion [12]. After the OFDM demodulation, two columns of data will be aggregated into one data sequence by the DSP module and then sent to the FSO transmitter. Since there are only two columns of VLC data, the OOK modulation is implemented in the FSO channel.

After the FSO channel transmission, the optical signal will be received by the APD, filtered, demodulated, amplified and sent to the DSP module, in which the data will be firstly separated to the two original data sequences, and then implemented the second-segment OFDM-based VLC transmission (VLC channel 2) whose steps are as same as those in the first-segment. The two columns of demodulated data will be finally sent to the oscilloscope (OSC, Lecroy 735Zi, 50 Ω) to analyze the transmission performance. Fig. 4 presents the photos of the experiment platform.

Two groups of experiments are implemented, and the first group evaluates the transmission performance of the VLC channels. The first-segment VLC system along with the FSO transmitter is deployed in one building of our campus, whereas the second-segment VLC system along with the FSO receiver is deployed in another building, shown in Fig. 4. The FSO transmitter and receiver are fixed and exactly aligned in the first group of experiments, and the LOS distance is 430 meters. There are altogether six FPGA boards (Xilinx V7 VC709) used in the whole platform for DSP

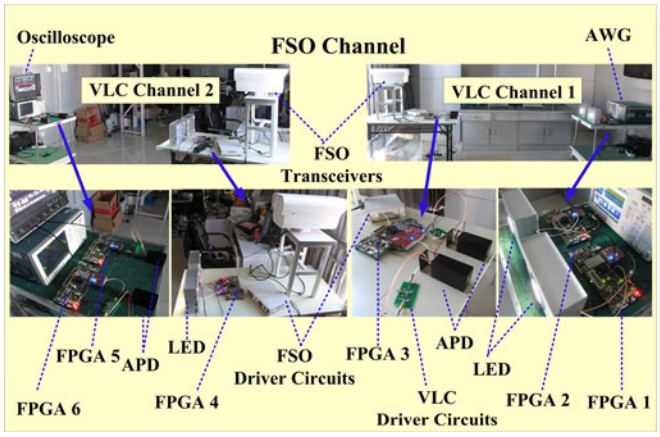

Fig. 4. FSO/VLC heterogeneous interconnection experimental platform.

TABLE I
OFDM Parameters

Parameter	Value
FFT size	1024
Number of subcarriers	128
Pilots locations	16, 32, 48, 64 . . .
CP length	32
DAC resolution	16-bit
DAC sampling rate	0.64 Gsps
ADC resolution	12-bit
ADC sampling rate	0.64 Gsps

operations, including OFDM modulation and data aggregation/distribution. Table I presents the key parameters in the FPGA-based OFDM system. We measure the frequency response of the VLC system, and the −10 dB bandwidth is 80 MHz after the hybrid time- frequency-domain equalization [12]. In the experiments, three different QAM orders are designed in the FPGA for OFDM modulation including QPSK, 16-QAM and 64-QAM. The FFT size is 1024, in which 32 points are used for CP. The OFDM sub-carrier number is 128, in which 120 sub-carriers are used for data transmission and 8 sub-carriers are used for pilots (After every 15 data-carried subcarriers, one pilot is inserted. Although more pilots lead to more accurate channel estimation, yet the transmission efficiency will decreased. In our platform we make a tradeoff based on practical measurement). The FPGA boards are operated in parallel structure, and two channels are used in the experiment. The DAC card provides one channel of 16-bit DAC at 0.64 Gsps and the ADC card provides one channel of 12-bit ADC at 0.64 Gsps. The linear interpolation and the MMSE algorithm are deployed for channel estimation, and the CAZAC sequences are used for timing synchronization. In order to fully occupy the bandwidth of the VLC system, the AWG generates two columns of pseudo-random data sequences at three different data-rates 150 Mb/s, 300 Mb/s, and 450 Mb/s, corresponding to three different QAM orders, respectively (the synchronization sequences are included, but the training sequences for the pilots are generated by the FPGA, which are not included in the

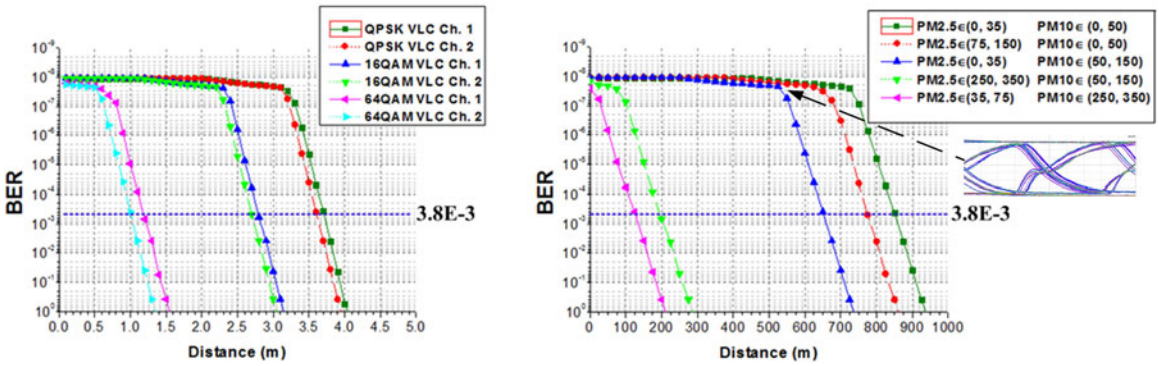

Fig. 5. (a) Transmission performance of the VLC-segments under different QAM levels. (b) Transmission performance of the FSO-segment under different weather conditions and the eye diagram.

AWG-generated data). For data aggregation and distribution, some identification bits are added into the aggregated data, and the total data-rates on the FSO link are 0.32 Gb/s, 0.64 Gb/s, and 0.96 Gb/s, respectively. The FSO transmit power is 8 dBm, and the receiver sensitivity is -36 dBm. The FSO transceiver operates at the wavelength 1550 nm and the divergence angle is 2 mrad.

The first group of experiments measures the system BER performance in different VLC transmission distances. In the experiments, the FSO transmission distance is fixed to 430 meters, whereas the VLC transmission distance is gradually increased from zero (both the transmission distances of the first-segment and the second-segment are changed simultaneously), and we measure and record the system BER every 10cm. Fig. 5(a) presents the results, which shows that the initial system BER is at the 10^{-8} level, which is mainly decided by the FSO channel and FPGA operation limits. When the VLC transmission distances originally change in a small range, the BER is relatively stable at 10^{-8} level, whereas the distances exceed a certain value, the BER is increasing significantly. Here we use the value of 3.8×10^{-3} as the BER threshold to determine the effective transmission distance, which is the typical limit for the efficient use of the FEC codes. Fig. 5(a) shows that the effective transmission distance of the first-segment VLC system is 3.7 meter, 2.9 meter, and 1.2 meter, corresponding to QPSK, 16-QAM and 64-QAM, respectively. Although the OFDM symbols are transmitting at the fixed rate of 80 Mb/s, the higher the QAM order, the shorter the transmission distance. On the other hand, the effective transmission distance of the second-segment VLC system is 3.6 m, 2.8 m, and 1.0 m, respectively. Although all the optical and electrical devices of the second-segment VLC system are as same as those in the first-segment, yet the results of the effective transmission distance are different. In our analysis, there are two reasons. The first is due to the differences of the signal quality before and after the FSO transmission, and the second reason lies in the environmental effects such as different ambient light of two VLC cells.

The second group of experiments evaluates the transmission performance of the FSO channel. The experimental platform is deployed in the outdoor environment. The AWG generates two columns of pseudo-random data sequences at the data-rate of 450 Mb/s, and the transmission speed of the FSO link is 0.96 Gb/s (with the 60 Mb/s additional identification bits generated by the FPGA for data aggregation). The transmission distances of the first and second VLC segments are fixed to 30 cm, whereas the FSO transmission distance is gradually increased from zero, and we measure and record the system BER every 25 m. The second group of experiments is implemented in five different non-turbulent (wind speed less than 2m/s) channel environments, in which the air quality, especially the values of particulate-matter (PM) 2.5 and PM10 are within five typical certain scales. In each channel condition, we implement the experiments four times and calculate the average values. Fig. 5(b) presents the experiment results along with the eye diagram, which show that the effective FSO transmission distances (BER is $3.8 * 10^{-3}$) under the five channel conditions

are 860 m, 770 m, 650 m, 190 m, and 120 m, respectively. Due to the practical limitations of the weather condition (The autumn and winter of the year 2016 is lack of rain and snow in Beijing), the FSO transmission performance in the rainy and snowy weather are not presented in the Fig. 5(b). Since there are only two columns of VLC data aggregated, the OOK-based FSO can realize efficient transmission, and if there are more columns of VLC data sequences involved, advanced modulation mechanisms will be required. The above experiments demonstrate the available performance for FSO/VLC heterogeneous interconnection and, therefore, validate the feasibility of the presented hybrid optical wireless network architecture.

4. Conclusion

We present a hybrid optical wireless network based on the FSO/VLC heterogeneous interconnection. This network is quite suitable to be deployed for the broadband wireless communication in RF-sensitive and security-required situations, especially in the deep-space, deep-ocean, and deep-ground environments for the future SAGO-integrated communication. Three different communication modes are defined in this network, along with the details for implementation. The FSO/VLC HetNet coordinator is the key element in this architecture, and we design its specific functional modules including both the physical-layer components and the network-layer mechanisms such as user identification and localization, user mobility and handoff control. We also build an experimental platform which firstly realizes a complete data aggregation/transmission/ distribution procedure based on FSO/VLC heterogeneous interconnection. Our future work includes enhancement and evaluation on the network-layer mechanisms, the improvement of the experimental platform such as APT modules and adaptive modulation and coding mechanisms, and the performance measurement in different turbulent environments.

References

[1] J. Reed, J. Bernhard, and J. Park, "Spectrum access technologies: The past, the present, and the future," *Proc. IEEE*, vol. 100, no. 5, pp. 1676–1684, May 2012.

[2] K. Tsukamoto, A. Hashimoto, Y. Aburakawa, and M. Matsumoto, "The case for free space," *IEEE Microw. Mag.*, vol. 10, no. 5, pp. 84–92, Aug. 2009.

[3] Z. Ghassemlooy, S. Arnon, M. Uysal, Z. Xu, and J. Cheng, "Emerging optical wireless communications—Advances and challenges," *IEEE J. Sel. Areas Commun.*, vol. 33, no. 9, pp. 1738–1749, Sep. 2015.

[4] H. Elgala, R. Mesleh, and H. Haas, "Indoor optical wireless communication: Potential and state-of-the-art," *IEEE Commun. Mag.*, vol. 49, no. 9, pp. 56–62, Sep. 2011.

[5] E. Ciaramella *et al.*, "1.28 terabit/s (32 x 40 Gbit/s) WDM transmission system for free space optical communications," *IEEE J. Sel. Areas Commun.*, vol. 27, no. 9, pp. 1639–1645, Dec. 2009.

[6] C. Abou-Rjeily and S. Haddad, "Cooperative FSO systems: Performance analysis and optimal power allocation," *J. Lightw. Technol.*, vol. 29, no. 7, pp. 1058–1065, Apr. 2011.

[7] H. AlQuwaiee, I. S. Ansari, and M. S. Alouini, "On the performance of free-space optical communication systems over double generalized gamma channel," *IEEE J. Sel. Areas Commun.*, vol. 33, no. 9, pp. 1829–1840, Sep. 2015.

[8] A. Garcíazambrana, C. Castillovázquez, B. Castillovázquez, and R. Boludaruiz, "Bit detect and forward relaying for FSO links using equal gain combining over gamma-gamma atmospheric turbulence channels with pointing errors," *Opt. Exp.*, vol. 20, no. 15, pp. 16394–16409, 2012.

[9] T. Komine and M. Nakagawa, "Fundamental analysis for visible light communication system using LED lights," *IEEE Trans. Consum. Electron.*, vol. 50, no. 1, pp. 100–107, Feb. 2004.

[10] A. Jovicic, J. Li, and T. Richardson, "Visible light communication: Opportunities, challenges and the path to market," *IEEE Commun. Mag.*, vol. 51, no. 12, pp. 26–32, Dec. 2013.

[11] J. Vucic, C. Kottke, S. Nerreter, K.-D. Langer, and J. W. Walewski, "513 Mb/s visible light communications link based on DMT-modulation of a white LED," *J. Lightw. Technol.*, vol. 28, no. 24, pp. 3512–3518, Dec. 2010.

[12] J. Li, Z. Huang, X. Liu, and Y. Ji, "Hybrid time-frequency domain equalization for LED nonlinearity mitigation in OFDM-based VLC systems," *Opt. Exp.*, vol. 23, no. 1, pp. 611–619, 2015.

[13] Y. Wang, Y. Wang, N. Chi, J. Yu, and H. Shang, "Demonstration of 575-Mb/s downlink and 225-Mb/s uplink bi-directional SCM-WDM visible light communication using RGB LED and phosphor-based LED," *Opt. Exp.*, vol. 21, no. 1, pp. 1203–1208, 2013.

[14] H. Haas, L. Yin, Y. Wang, and C. Chen, "What is LiFi?" *J. Lightw. Technol.*, vol. 34, no. 6, pp. 1533–1544, Mar. 2016.

[15] H. Burchardt, N. Serafimovski, D. Tsonev, S. Videv, and H. Haas, "VLC: Beyond point-to-point communication," *IEEE Commun. Mag.*, vol. 52, no. 7, pp. 98–105, Jul. 2014.

[16] P. H. Pathak, X. Feng, P. Hu, and P. Mohapatra, "Visible light communication, networking, and sensing: A survey, potential and challenges," *IEEE Commun. Surv. Tuts.*, vol. 17, no. 4, pp. 2047–2077, Oct.—Dec. 2015.

[17] Y. Li, N. Pappas, V. Angelakis, M. Pióro, and D. Yuan, "Optimization of free space optical wireless network for cellular backhauling," *IEEE J. Sel. Areas Commun.*, vol. 33, no. 9, pp. 1841–1854, Sep. 2015.
[18] L. Kong, W. Xu, L. Hanzo, H. Zhang, and C. Zhao, "Performance of a free-space-optical relay-assisted hybrid RF/FSO system in generalized M-distributed channels," *IEEE Photon. J.*, vol. 7, no. 5, pp. 1–19, Oct. 2015.
[19] L. Chen, W. Wang, and C. Zhang, "Multiuser diversity over parallel and Hybrid FSO/RF links and its performance analysis," *IEEE Photon. J.*, vol. 8, no. 3, pp. 1–10, Jun. 2016.
[20] J. Song, W. Ding, F. Yang, H. Yang, B. Yu, and H. Zhang, "An indoor broadband broadcasting system based on PLC and VLC," *IEEE Trans. Broadcast.*, vol. 61, no. 2, pp. 299–308, Jun. 2015.
[21] Y. Wang, J. Shi, C. Yang, Y. Wang, and N. Chi, "Integrated 10 Gb/s multilevel multiband passive optical network and 500 Mb/s indoor visible light communication system based on Nyquist single carrier frequency domain equalization modulation," *Opt. Lett.*, vol. 39, no. 9, pp. 2576–2579, 2014.
[22] M. Kashef, M. Ismail, M. Abdallah, K. A. Qaraqe, and E. Serpedin, "Energy efficient resource allocation for mixed RF/VLC heterogeneous wireless networks," *IEEE J. Sel. Areas Commun.*, vol. 34, no. 4, pp. 883–893, Apr. 2016.
[23] M. B. Rahaim and T. D. C. Little, "Toward practical integration of dual-use VLC within 5G networks," *IEEE Wireless Commun.*, vol. 22, no. 4, pp. 97–103, Aug. 2015.
[24] S. Buzzi, C.-L. I, T. E. Klein, H. Vincent Poor, C. Yang, and A. Zappone, "A survey of energy-efficient techniques for 5 G networks and challenges ahead," *IEEE J. Sel. Areas Commun.*, vol. 34, no. 4, pp. 697–709, Apr. 2016.
[25] Z. Zheng, L. Liu, T. Chen, and W. Hu, "Integrated system of free-space optical and visible light communication for indoor wireless broadband access," *Electron. Lett.*, vol. 51, no. 23, pp. 1943–1944, 2015.
[26] Y. Liu, Z. Huang, W. Li, and Y. Ji, "Game theory-based mode cooperative selection mechanism for device-to-device visible light communication," *Opt. Eng.*, vol. 55, no. 3, pp. 030501-1—030501-4, 2016.
[27] Z. Huang, C. Yan, K. Wu, and Y. Ji, "Indoor multi-robot intelligent coordination based on omni-directional visible light communication," *Chin. Opt. Lett.*, vol. 14, no. 10, pp. 102301-1–102301-5, 2016.
[28] R. Zhao, Z. Huang, Y. Liu, and Y. Ji, "United block sequence mapping-based visible light positioning for dense small cell deployment," *Chin. Opt. Lett.*, vol. 14, no. 7, pp. 070601-1—070601-6, 2016.
[29] Z. Huang, J. Xiong, J. Li, and Y. Ji, "Efficient cross-room switch mechanism for indoor room-division-multiplexing based visible light communication network," *J. Opt. Soc. Korea*, vol. 19, no. 4, pp. 351–356, 2015.
[30] Z. Huang and Y. Ji, "Design and demonstration of room division multiplexing-based hybrid VLC network," *Chin. Opt. Lett.*, vol. 11, no. 6, pp. 16–20, 2013.